

End-to-end delay analysis in an Integrated Modular Avionics architecture

Nesrine Badache, Katia Jaffrès-Runser, Jean-Luc Scharbag, Christian Fraboul
University of Toulouse IRIT-INPT/ENSEEIH

2, rue Camichel, 31000 Toulouse, France

Nesrine.Badache, Katia.Jaffres-Runser, Jean-Luc Scharbag, Christian.Fraboul@enseeiht.fr

Abstract

Recent modular avionics architectures have been designed to share computation and communication resources. However, such an approach creates new challenges to master the temporal properties of avionics applications.

In the context of IMA (Integrated Modular Avionics), it is crucial to investigate the performance gains that future integration platforms and software will propose. This paper brings to light the impact of spatial and temporal integration choices on the communication performance (e.g. message loss rate, latencies, ...). The conclusion of this investigation is that it is necessary to conduct a thorough modeling and simulation study of an IMA architecture integrating several applications during its early design stages.

1. Introduction

Embedded avionics systems have evolved from a federative architecture where calculators were interconnected through dedicated mono-emitter links [2] towards a modular architecture. The Integrated Modular Avionics (IMA) has been standardized as ARINC 651 standard [4] for the definition of the hardware architecture and as ARINC 653 [5] for the corresponding software architecture. They define the APEX (APplication EXecutive interface) which ensures the spatial and temporal partitioning of the avionics functions. Thus, it is possible to design the application software independently from the target IMA physical platform.

However, such a modular architecture still necessitates a thorough configuration step at the early stages of its design, both at the physical and software levels. The first point in this article is to evaluate the impact of such configuration and integration choices on the overall performance of the system. Indeed, sharing communication and computation resources in such a modular system increases the complexity of accounting for the temporal properties of the target avionics applications (e.g. execution frequency of functions, communication delays, ...). More specifically, we show that the core of this problem is to evaluate end-to-end communication delays between remotely located and distributed avionics functions.

This article is organized as follows. Section 2 presents

the relevant assumptions for the integration of avionics applications on an IMA architecture, centered around an AFDX network. In Section 3, the impact of integration choices on end-to-end communication performance is illustrated on an example architecture. Section 4 presents the proposed modeling and simulation strategy to compare the communication performance of different architectures for different integrations and configuration choices. Concluding remarks and future works are given in Section 5.

2. IMA applications integration

An IMA architecture interconnects several computation modules, sensors and actuators using one or more communication networks. Computation modules communicate mainly using an AFDX network (Avionic Full Duplex Switched Ethernet) which has been standardized in ARINC 664 [6]. AFDX relies on a switched Ethernet technology and provides communication means for asynchronous computation modules. Data is transmitted using the so-called virtual links (VLs) that ensure data flow segregation. A VL defines a mono-emitter logical communication path through a sequence of switches. It is characterized by the minimum time that separates two consecutive frames transmitted by the same source, referred to as the BAG (Bandwidth Allocation Gap) and a maximum frame size SMAX.

An avionics application is composed of a set of functions or tasks, which are executed in partitions that ensure the temporal and physical segregation between applications. These partitions communicate using ports and logical APEX channels. Partitions are executed periodically on the physical modules and are statically scheduled in a cyclical frame called MAF (MAJOR time Frame). A partition hosts a set of periodic or aperiodic tasks that are scheduled based on a pre-defined policy. Two types of APEX ports exist: sampling and queuing ports. In a sampling port, a new piece of data overwrites the previously stored one, whether the old one has been consumed (i.e. read) or not. In contrast, in a queuing port, all incoming pieces of data are stored in their order of arrivals.

In the design of an IMA system, the problem is then to allocate the partitions to the computation modules (spatial allocation), to allocate the APEX channels for the various communications taking place between the tasks and to define appropriate MAFs (temporal allocation). This integration has to guaranty that end-to-end communica-

tion delays or packet losses are maintained below given limits.

This integration problem is illustrated for the application presented in Figure 1. This application is composed of 14 partitions P_1, P_2, P_{14} . Each partition $P_i, 1 \leq i \leq 7$, executes a periodical function F_i . At the end of its execution, each function (i.e. task) F_i creates a message Msg_i to be sent to function F_{i+7} . In this example, functions F_1 to F_6 have a period of $32ms$ while F_7 has a period of $16ms$.

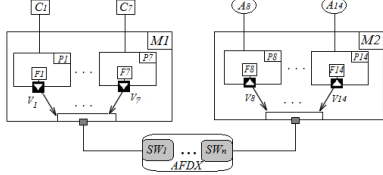


Figure 1. Illustrative IMA example.

The target physical architecture for this application is composed of computation modules interconnected via an AFDX network. A first module M_1 is linked to sensors C_1 to C_7 whose values are read by functions F_1 to F_7 , respectively. These functions are hosted by partitions P_1 to P_7 , which are executed in module M_1 . A second module M_2 is linked to a set of actuators A_1 to A_7 which are commanded by functions F_8 to F_{14} . Partitions P_8 to P_{14} are executed on module M_2 for functions F_8 to F_{14} , respectively.

Functions $F_i, 1 \leq i \leq 7$, communicate with its remote functions F_{i+7} by sending at the end of each one of their activation period a message Msg_i . The resulting seven message flows are transmitted from module M_1 to M_2 using seven VLs, V_1, \dots, V_7 , defined in the AFDX port of M_1 (Msg_i is sent on V_i). We assume that the size of a message does not exceed the maximum packet size of its VL. A reasonable design for the MAFs of M_1 knowing the periodicity of F_1 to F_7 is to create a MAF of $14ms$ repeating itself every $16ms$. Each function is executed during $2ms$. The MAF of M_1 is thus subdivided into 7 slots of $2ms$ each (cf. Figure 2).

The first six slots are used every two MAF cycles (i.e. every $32ms$) by F_1 to F_6 , while slot number seven is used each cycle (i.e. every $16ms$) by F_7 . Accordingly, VLs V_1 to V_6 are assigned a BAG of $32ms$ and V_7 a BAG of $16ms$.

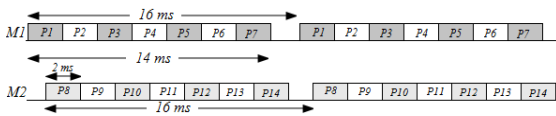


Figure 2. MAFs of modules M_1, M_2

The MAF of module M_2 follows the same model as M_1 as shown in Figure 2. M_1 and M_2 modules are asynchronous, which means that MAFs can experience different offsets as the physical module is being started. Unfortunately, no simplifying assumption can be made regarding these offsets.

3. Impact of applications integration

This section investigates the impact of integration choices on end-to-end communication performance. To this end, we first define the end-to-end communication delay. Then, we show on the example of figure 1 how integration choices impact these delays.

In our analysis, we derive the end-to-end communication delay of the function F_7 that transmits the messages Msg_7 to the function F_{14} through VL V_7 . The end-to-end communication latency is here defined as the duration between the time Msg_7 is generated in F_7 and the time it has been consumed by F_{14} . It is decomposed into three components:

– $T_{VL}:Msg_7$ has to wait until a BAG has elapsed before being transmitted on the VL. T_{VL} is the time Msg_7 is waiting for an available transmission slot in V_7 . T_{VL} varies from $0ms$ to V_7 BAG size.

– T_{nw} : the latency the message experiences in the network. It is completely determined by the target network properties.

– T_{dest} : When Msg_7 arrives at the incoming port of M_2 , it has to wait until function F_{14} is scheduled and can consume it. Thus, T_{dest} is the duration Msg_7 has to wait in M_2 before being read by its destination function. These

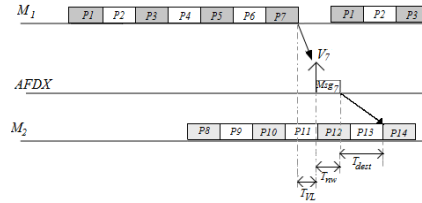


Figure 3. F_7 and F_{14} communication

communication latencies are illustrated on our example in the following:

1. **Latency for an available VL slot.** In the example of figure 3, the MAF of M_1 and VL V_7 have an equal period ($16ms$). In this case, T_{VL} is constant for each new message instance (cf. T_{VL} on figure 3). Now, what happens if the period of a function F_x does not match with a possible BAG value (BAGs values are limited to powers of two durations, starting at $8ms$)? Let consider a period for F_x of $30ms$. The corresponding partition can be allocated in a $30ms$ MAF cycle. To ensure the availability of a BAG of the VL V_x from each message production, the BAG size has to be fixed to the largest available BAG size which is lower or equal to F_x period, i.e. $16ms$ in this case. Thus, a message created every $30ms$ finds an available slot for transmission in the VL of period $16ms$.

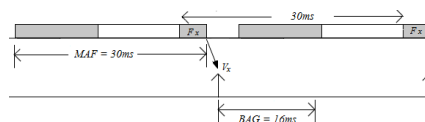


Figure 4. Availability in V_x

Consequently, it is possible to control the latency for the VL availability (as long as the message sending period is not lower than the smallest BAG i.e $1ms$).

- Latency through the network.** The latency T_{nw} consists in two parts: *i*) the multiplexing delay d_{mux} on the M_1 output port and *ii*) the transmission latency T_p through the network.

a) Multiplexing delay d_{mux} : all the VL data frames are multiplexed in an ordered sequence according to the messages sending times in the AFDX port. Thus, a data frame of V_7 arrived after a set of data frames produced earlier by other VLs will have to wait for complete transmission of previous frames. This multiplexing delay is depicted in figure 5 for three successive frames of V_7 of the illustrative example. All VLs carry here a frame size of 1530 bytes. At 100 Mbps, emission duration is of $0.122ms$. The activation of the function F_1 to F_6 during the first occurrence causes a delay of $0.732ms$ for the data frame of V_7 . Considering the previously defined BAG values ($16ms$ for V_7 , $32ms$ for V_1 to V_6), the same behavior is repeated in the third occurrence in V_7 . However, the second occurrence of V_7 is not affected ($d_{mux} = 0$). The difference between the minimum and the maximum d_{mux} value is denoted by *multiplexing jitter*. When the data frames generation times of the VLs are at the source module (e.i. modules and VLs offsets are known), this multiplexing jitter can be analytically computed [9], otherwise, it requires a recursive derivation through simulations.

b) Transmission latency through the AFDX network: it is the difference between the data frame release time from the output of the source module and the reception time in the destination module. In an AFDX network, this delay varies depending on the network traffic [10]. Different approaches to bound this variability exist [10]. Some approaches take into account the local scheduling of different VLs originating from the same source. It has also been shown that this local scheduling of VLs can significantly reduces the delays occurred in the network [11].

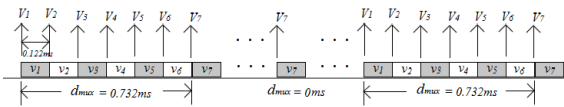


Figure 5. Multiplexing delay in V_7

- Latency at the destination module.** The variation in the latency T_{nw} means that the successive data frames received in destination module M_2 are no longer periodic. This is illustrated in figure 6.

The function F_{14} is periodic. However, the variable latency introduced by the AFDX network on Msg_7 occurrences results in an additional delay T_{dest} on the reception time in the destination module. Since M_1 and M_2 are asynchronous, it is impossible to set execution times of P_{14} on M_2 to compensate for this network jitter.

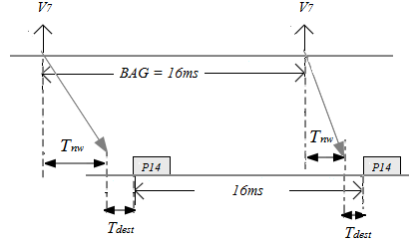


Figure 6. Latency at the destination module M_2

It is therefore possible that two data frames of V_7 arrive between two successive executions of P_{14} . This scenario is shown in the figure 7.

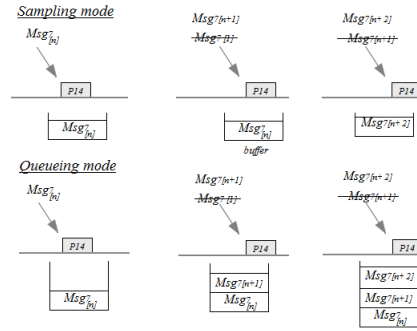


Figure 7. Reception in sampling and queueing modes

Depending on the type of destination port (queuing or sampling), such successive data receptions have a consequence on the communication performance. The message Msg_{7n+1} overwritten by the new occurrence Msg_{7n+2} . If it is a queueing port, the message Msg_{7n+1} is consumed in the next execution of P_{14} ($n+2$). In this case, $T_{dest} > 16ms$. To avoid such loss of messages or additional delay problems, the execution period of P_{14} has to be reduced to avoid the reception of two successive data frames on M_2 is determined by deducting the multiplexing jitter induced by the network ($T_{nw} = T_{mux} + T_p$ in this case) from the execution period of P_{14} . The figure 8 illustrates the minimal required duration avoid messages loss (sampling) or additional delay (queueing).

4. Proposed modeling and simulation tool

The analysis of Section 3 stresses the need for a tool capable to evaluate and compare different integration choices. Such a tool would enable the comparison and optimization of the temporal and spatial allocations needed in the design of an IMA system. For example,

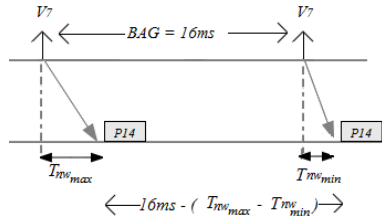


Figure 8. Minimal execution period

it could provide optimal MAF constructions for remotely communicating applications, under given end-to-end requirements. Likewise, is needed compare the parameters of different communication architectures by changing for example the number and the characteristics of VLs (BAG, SMAX) in an AFDX network. This comparison can consider different priority levels among messages (messages loss and additional delay not allowed), or messages with less strict constraints. Overall, it is about the comparison of different IMA platform architectures (number of modules, AFDX ports, ...) that lead to different allocation spatial scenarios.

Our main objective is the modeling and simulation of an IMA platform. It consists in the description of the different characteristics (software architecture, physical architecture, integration), to generate a simulation model able to verify the application constraints and requirements. The proposed modeling approach is described in the figure 9. It consists of three modeling levels: application model, architecture model and integration model.

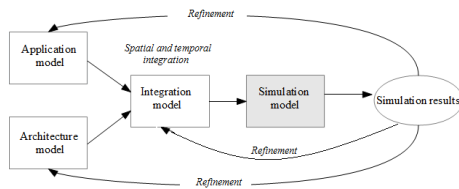


Figure 9. Proposed modeling approach

The application model describes the avionics applications in term of communicating partitions across logical communication ports and APEX channels. It also describes the embedded functions embedded onto the partitions.

The architecture model formalizes the description of an IMA platform architecture in terms of physical components (execution modules, sensors, actuators, ...) linked in heterogeneous networks.

The integration model describes the mapping of the application model onto the architecture model: spatial allocation of the partitions onto the execution modules and the APEX channels on the AFDX ports, and the temporal allocation of partitions and modules (MAF) and the virtual communication links (BAGs, SMAX).

The auto-generated simulation model is obtained from the integration model which is capable of driving the performance of the loaded IMA architecture. with respect to different communication metrics (end-to-end communication delay, jitters, messages loss, ...)

The generated simulation model can be used to evaluate the performance of application and architecture models. Moreover, we can use these results to fine tune the parameters defined in application and architecture model and re-generate the simulation model.

This iterative process can help in early design phase to decide optimal parameters for the IMA architecture. We are developing such a tool and initial results are encouraging.

5. Conclusion

In this paper we have presented the complexity of communication delays, analysis in the context of IMA architecture (impact of the multiplexing jitter and the communication in sampling and queueing modes, influences of source and destination execution periods and influence of the choice of the logical communication channels).

A deep analysis of those influential parameters requires a simulation tool able to consider the random aspects (offsets of the modules and networks, tasks execution duration, communication delay, ...).

The ongoing research covers the modeling approach of such an IMA architecture according to three levels (application, architecture, integration) and aims at generating a simulation tool that can be used to calculate the end-to-end communication of modeled software and physical architecture.

References

- [1] M. Lauer and al. : *Latency and freshness analysis on IMA systems*. ETFA 2011, Toulouse, France, Sep. 2011.
- [2] Aeronautical Radio Inc. ARINC 429, *ARINC specification 429-ALL: Mark 33 Digital Information Transfer System*, 2001.
- [3] F. Martin and C. Fraboul : *Modeling and Simulation of Integrated Modular Avionics* PDP 1998, Madrid, Spain, January 1998.
- [4] Aeronautical Radio Inc. ARINC 651, *Design Guidance for Integrated Modular Avionics*, 1991.
- [5] Aeronautical Radio Inc. ARINC 653, *Avionics Application Software Standard Interface*, 1997.
- [6] Aeronautical Radio Inc. ARINC 664, *Aircraft Data Network, Part 7: Avionics Full Duplex Switched Ethernet (AFDX) Network*, 2005.
- [7] M. Lauer and al. : *Analyzing end-to-end functional delays on an IMA platform*. In Proc. of the 4th ISO/LA'10, Heraklion, Greece, page 243-257. Springer-Verlag, 2010.
- [8] J. Javier Gutiérrez and al. : *Response time analysis in AFDX networks with sub-virtual links and prioritized switches*. JTR'12, Santander, Spain, January 2012.
- [9] A. Choquet-Geniet and E. Grolleau : *Minimal schedulability interval for real time systems of periodic tasks with offsets*. Theoretical of Computer Sciences, vol. 310, pp. 117-134, 2004.
- [10] H. Bauer and al. : *Worst-case delay analysis of an industrial AFDX network* DATE 2011, Dresden, Germany, Mars 2013.
- [11] X. Li and al. : *Existing offset assignments are near optimal for an industrial AFDX network* RTN 2011, Porto, Portugal, July 2011.